International Journal of Power Electronics and Drive System (IJPEDS)
Vol. 17, No. 4, December 2026, pp. 2382~2392
ISSN: 2088-8694, DOI: 10.11591/ijpeds.v17.i4.pp2382-2392

Ion motion algorithm-based MPPT for photovoltaic systems using a SEPIC converter under partial shading conditions

Endro Wahjono, Indhana Sudiharto, Farah Izdihar Nakha Aqilah
Department of Industrial Electrical Engineering, Electronic Engineering Polytechnic Institute of Surabaya, Surabaya, Indonesia

Article Info

Article history:

Received Jul 10, 2026
Revised Aug 18, 2026
Accepted Sep 17, 2026

Keywords:

Ion motion optimization algorithm
Maximum power point tracking
Partial shading
Particle swarm optimization
Photovoltaic systems
SEPIC converter

ABSTRACT

Solar photovoltaic (PV) output depends heavily on the prevailing irradiance, and once shading becomes non-uniform, the power-voltage (P-V) curve can break into several local peaks alongside a single true maximum, a situation that frequently defeats conventional maximum power point tracking (MPPT) schemes searching for the global maximum power point (GMPP). To address this limitation, this paper presents an MPPT strategy built on the Ion motion optimization algorithm (IMOA) and paired with a SEPIC DC-DC converter for stand-alone (off-grid) PV systems. The controller was assessed through closed-loop simulations in PSIM across four irradiance levels: 1000 W/m², 750 W/m², 500 W/m², and 250 W/m². Under uniform, full irradiance, the algorithm delivered an output power of 95.08 W, a tracking accuracy of 99.77%, and a tracking time of 0.98 s; under partial shading, it sustained an accuracy above 99% while converging faster than a benchmark particle swarm optimization (PSO) controller. These findings indicate that the proposed IMOA-based approach reliably and effectively locates the GMPP across changing irradiance conditions.

This is an open access article under the CC BY-SA license.

Corresponding Author:

Indhana Sudiharto
Department of Electrical Engineering, Industrial Electrical Engineering
Electronic Engineering Polytechnic Institute of Surabaya
Raya ITS – PENS Campus, Sukolilo, Surabaya 60111, Indonesia
Email: indhana@pens.ac.id, indhanasudiharto@gmail.com

1. INTRODUCTION

Among renewable energy options, photovoltaic (PV) technology stands out for its ability to convert sunlight directly into electricity [1], and the growing push for cleaner power generation has driven PV deployment into an expanding range of applications. Yet how well a PV system performs is tightly coupled to its operating environment, particularly irradiance and temperature, because the underlying electrical behavior of a PV module is fundamentally nonlinear and therefore yields output power that shifts continuously as conditions change. Specifically, irradiance swings of roughly 250–1000 W/m² mainly alter the generated current and power, whereas temperature increases in the 54–66 °C range tend to pull the output voltage down; both effects move the maximum power point (MPP) along the power–voltage (P–V) curve [2], [3].

Real-world PV installations rarely receive perfectly even sunlight; passing clouds, nearby structures, trees, or dust buildup on the module surface routinely create what is known as partial shading. Once shading becomes uneven, the P–V curve no longer shows a single hump but instead splits into one global maximum power point (GMPP) accompanied by several local maximum power points (LMPP), and telling the global peak apart from the local ones is precisely what makes the tracking task harder. Classical maximum power point tracking (MPPT) approaches such as perturb and observe (P&O) and incremental conductance (INC) are prone to settling on a local peak rather than the global one under these conditions, which lowers the power actually harvested and degrades overall system efficiency [4]-[6].

In response to these challenges, researchers have turned to metaheuristic optimization as a basis for more capable MPPT controllers. Methods such as particle swarm optimization (PSO), genetic algorithm (GA), and related evolutionary techniques have shown they can outperform conventional tracking under demanding, fast-changing conditions, largely because their global search behavior helps them escape local maxima. Even so, one optimizer that has received comparatively little attention in this context is the ion motion optimization algorithm (IMOA); its use for PV MPPT, particularly under partial shading, remains largely unexplored.

Existing metaheuristic MPPT studies, including PSO, genetic algorithm, and their more recent hybrid or improved variants [7], [8], generally attain global tracking at the cost of slower convergence, sensitivity to tuning parameters, or added computational overhead, which limits their responsiveness under rapidly changing partial-shading patterns. IMOA has not previously been evaluated for this problem, and its two-stage liquid-crystal search behavior offers a plausible route to faster convergence without sacrificing tracking accuracy. This gap between the demonstrated capability of IMOA in general optimization tasks and its absence from the PV MPPT literature is the specific problem this study addresses. Accordingly, the novelty of this work lies not in proposing a new optimization algorithm, but in being the first to adapt and evaluate IMOA as an MPPT controller for a SEPIC-based PV system under partial shading, and in benchmarking it directly against PSO under matched simulation conditions to quantify the practical benefit of the exploration-exploitation mechanism described above.

IMOA is a population-based metaheuristic whose search behavior is drawn from the way oppositely charged ions attract and repel one another. Because this mechanism gives it both a wide-ranging global search and comparatively rapid convergence, it is well matched to nonlinear optimization problems of the kind posed by multi-peak MPPT under partial shading [9]. Pairing the controller with a single-ended primary inductor converter (SEPIC) adds further flexibility, since this converter topology can step the voltage up or down without inverting its polarity, a trait well suited to the fluctuating output of a PV array under changing environmental conditions [10].

Building on this rationale, the present study combines an IMOA-based controller with a SEPIC converter to improve power extraction when shading is non-uniform. Three contributions are offered: first, IMOA is implemented and applied to PV MPPT under non-uniform irradiance; second, the resulting system is assessed for convergence speed, tracking accuracy, and stability; and third, its performance is benchmarked against a conventional, widely used MPPT method to gauge the practical benefit of the proposed approach.

2. METHODOLOGY

To improve the energy yield of a PV system, an MPPT controller built around the ion motion optimization algorithm (IMOA) is implemented here. The hardware arrangement comprises a PV module, a DC–DC SEPIC converter, and a microcontroller unit running the IMOA-based MPPT routine, as illustrated by the block diagram in Figure 1. A simulation-based research design was adopted for this study. This approach was chosen because it allows the IMOA and PSO controllers to be evaluated under identical, precisely repeatable irradiance conditions - including uniform and three partial-shading patterns - which is difficult to guarantee consistently on an outdoor hardware testbed, and because it lets the two algorithms be compared strictly on their tracking behavior rather than on differences in sensor noise or hardware tolerances. The overall workflow proceeded in four stages: i) Modelling the PV module and validating its I-V/P-V behavior against the manufacturer datasheet values in Table 1; ii) Designing the SEPIC converter components in Table 2 to keep the converter in continuous conduction mode; iii) Implementing the IMOA and PSO controllers as C-block routines within the closed-loop PSIM circuit shown in Figure 2; and iv) Evaluating both controllers under the irradiance patterns in Table 3, using tracking accuracy, tracking time, and output power as the comparison metrics.

Figure 1 depicts the system block diagram together with the operating logic of the ion motion optimization algorithm used for tracking the maximum power point. Movement through the search space is driven by the attraction and repulsion between positively and negatively charged ions, which lets the algorithm explore broadly while still converging on a stable result; this combination helps IMOA steer clear of local maxima and home in on the true global maximum power point [9]. For a PV array built from two 50 Wp panels, shifting irradiance and temperature can give rise to several local peaks on the P–V curve once shading becomes uneven [4]. Relative to conventional schemes such as P&O and incremental conductance (INC), IMOA converges faster and tracks more accurately, qualities that make it a reasonable candidate for real-time MPPT in systems with multiple PV panels.

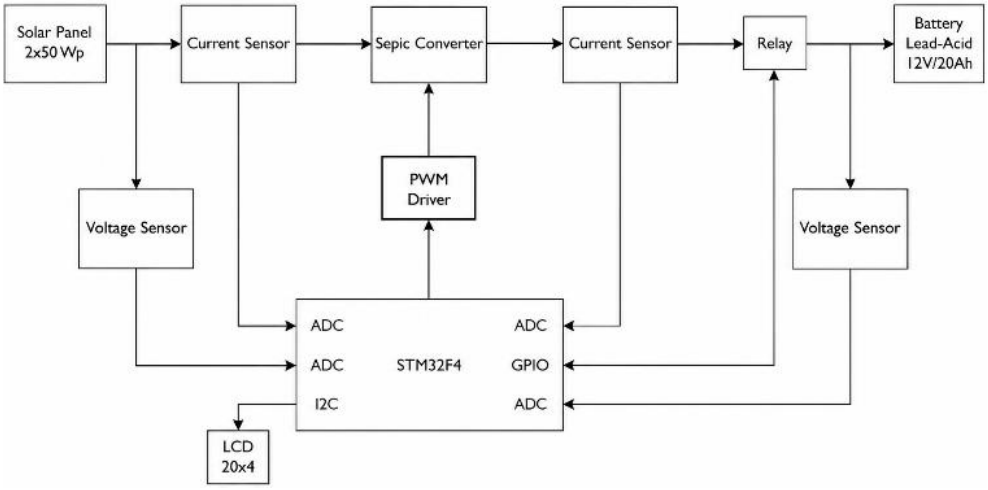

Figure 1. System diagram block

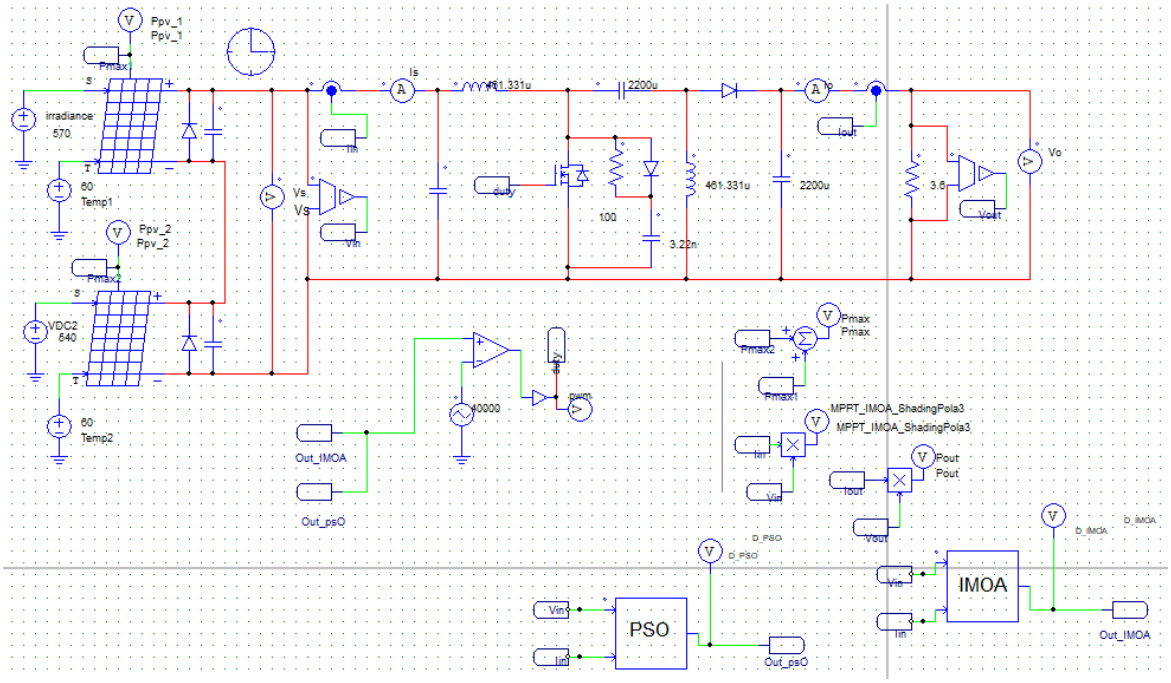

Figure 2. Simulation setup in PSIM

Table 1. Specifications of the solar cell

Component	Value
P_{max}	50 W
V_{mpp}	18 V
I_{mpp}	2.78 A
V_{oc}	22.11 V
I_{sc}	2.94 A

Table 2. Specifications of the SEPIC converter

Component	Value	Component	Value
L_1 (Inductor 1)	461.331 μH	$C_{snubber}$ (capacitor snubber)	3.3 nF
L_2 (Inductor 2)	461.331 μH	$R_{snubber}$ (resistor snubber)	553 Ω
C_1 (Capacitor 1)	1979 μF	Frequency switching	40 kHz
C_2 (Capacitor 2)	1979 μF		

Table 3. GMPP AND LMPP values of each pattern

Pattern	Irradiance (W/m²)		GMPP (W)	LMPP (W)
	PV module 1	PV module 2		
Partial shading 1	1000	750	37.32	21.64
Partial shading 2	1000	500	35.76	21.49
Partial shading 3	1000	250	33.30	21.44

2.1. Photovoltaic PV module

A PV module is built from semiconductor solar cells that convert sunlight into electricity through the photovoltaic effect, with individual cells wired in series and parallel combinations to reach the desired voltage and current ratings. Because the resulting output is nonlinear, it responds strongly to surrounding environmental factors such as irradiance and temperature [11]. This behavior is commonly modeled with an equivalent circuit consisting of a current source, a diode, and a pair of internal resistances. Within that model, the output current is governed chiefly by the photo-generated current and the diode's own characteristics, both of which vary with irradiance and temperature, giving rise to the familiar nonlinear current–voltage (I–V) and power–voltage (P–V) profiles seen across different operating conditions [3], [11].

$$I = I_{ph} - I_0\left(e^{\frac{V}{nV_t}-1}\right) - \frac{V+IR_S}{R_{sh}} \quad (1)$$

Here, I and V denote the PV module's output current and voltage, I_{ph} is the current produced by incident sunlight, I_0 is its diode saturation current, R_s and R_{sh} are its series and shunt resistances, and nV_t denotes the thermal voltage. These parameters together account for the nonlinear I–V and P–V behavior described above [3], [11]. As the irradiance level increases, the output current and power increase roughly in proportion, while a temperature rise instead pulls the output voltage down. The net effect is that the MPP keeps drifting, which is why a dedicated maximum power point tracking (MPPT) control technique is needed to keep the system operating optimally [12]. When irradiance is uniform, the P–V curve has just one peak, marking the MPP; but once shading is uneven, mismatched cell-level operating conditions give rise to additional peaks, so the curve ends up with one GMPP and several LMPPs. This added complexity is what makes the MPPT process harder to solve correctly [4], [13].

A solid grasp of these PV module characteristics is therefore a prerequisite for designing MPPT algorithms that remain efficient under dynamic, non-uniform environmental conditions. Table 1 lists the electrical ratings of the PV module used in this study: a maximum power P_{max} of 50 W, an MPP voltage and current of V_{mpp} = 18 V and l_{mpp} = 2.78 A, along with an open-circuit voltage V_{oc} = 22.11 V and a short-circuit current I_{sc}= 2.94 A. These figures establish the module's operating envelope and underpin both the PV model and the design of the MPPT controller and DC–DC converter, ensuring reliable performance across changing conditions [11].

2.2. Maximum power point tracking

MPPT refers to the control strategy that keeps a PV system extracting as much power as possible despite changing environmental conditions. Since irradiance and temperature shifts move the MPP along the nonlinear P–V curve [13], [14], a system left without MPPT control will tend to drift away from that point, converting energy less efficiently. P&O and incremental conductance (INC) remain popular precisely because they are straightforward to implement, yet both tend to oscillate around the MPP and lose effectiveness when irradiance changes quickly or shading creates several local maxima on the P–V curve [15], [16]. This is why MPPT, through its regulation of the DC–DC converter's duty cycle, is so central to keeping a PV system — especially an off-grid one operating close to the global maximum power point.

Figure 3 plots the typical I–V and P–V characteristics of a PV module: The I–V curve traces how current relates to voltage, while the P–V curve traces how power varies, with its peak, the MPP, marking the module's optimal operating point [8], [9]. When irradiance differs from one PV module to another, the array's P–V curve can break into several peaks rather than one, again yielding a single GMPP alongside multiple LMPPs, which adds to the difficulty of the MPPT task. Knowing where the GMPP and LMPP fall under each shading pattern matters because it serves as the benchmark against which the proposed algorithm's ability to distinguish global from local optima is judged. Table 3 lists the irradiance combinations examined in this study along with their corresponding GMPP and LMPP values.

Table 3 summarizes how the simulated output changes with irradiance: power falls steadily as irradiance drops from 1000 W/m² to 250 W/m², consistent with the expected behavior of photovoltaic systems. Even with this drop in available power, the IMOA-based controller continues to track accurately and consistently. It adjusts the SEPIC converter's duty cycle so that operation stays close to the MPP even at low irradiance, where the P–V curve flattens out and becomes harder to follow.

2.3. Ions motion optimization algorithm (IMOA)

IMOA is a population-based metaheuristic that takes its inspiration from how ions behave physically in nature. It models a population of charged particles — anions, which carry a negative charge, and cations, which carry a positive one — following the basic electrostatic rule that like charges repel and

opposite charges attract. To balance broad exploration of the search space against focused exploitation of promising regions, the algorithm proceeds through two stages: the liquid phase and the crystal phase [9].

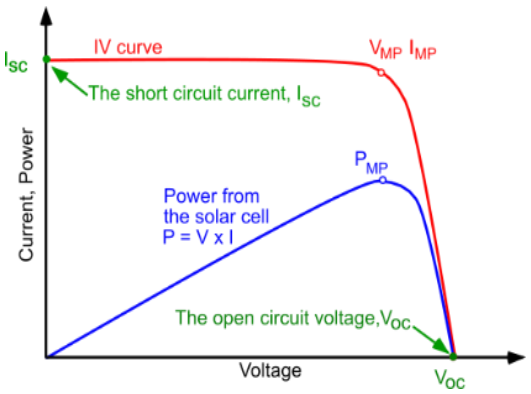

Figure 3. Typical current–voltage (I–V) and power–voltage (P–V) curves of a photovoltaic module indicating the maximum power point (MPP)

a) Liquid phase (diversification)

During the liquid phase, the ions move freely, which lets the algorithm range widely over the search space. Here, each ion is drawn primarily toward the best-performing ion of the opposite charge, and a sigmoid function is used to compute the resulting attraction forces for anions (AF) and cations (CF) so that convergence stays stable [15].

$$AF_{i,j} = \frac{1}{1+e-0.1/AD_{i,j}} \quad (2)$$

$$CF_{i,j} = \frac{1}{1+e-0.1/CD_{i,j}} \quad (3)$$

Where $AD_{i,j}$ denotes the distance separating the i-th anion and the best cation (Cbest) in the j-th dimension, while $CD_{i,j}$ denotes the distance separating the i-th cation and the best anion (Abest). Ion positions are then updated as (4) and (5).

$$dA_{\mathrm{i,j}} = dA_{i,j} + AF_{i,j} \text{ x } Cbest_j - dA_{i,j} \quad (4)$$

$$dC_{\mathrm{I,j}} = dC_{i,j} + CF_{i,j} \text{ x } Abest_j - dC_{i,j} \quad (5)$$

b) Crystal phase (intensification)

Once the ion population begins to stabilize, the algorithm switches into the crystal phase to speed up convergence toward the global optimum. Position updates in this phase rely on a random factor ∅ drawn from the interval [-1, 1], used to search the immediate neighborhood of the current best solutions:

$$\begin{aligned}
&if\ (CbestFit >= CworstFit\ /\ 2\ and\ AbestFit >= AworstFit\ /\ 2)\\
&\quad if\ rand\ () > 0.5\\
&\qquad A_i = A_i + \emptyset_1\ x\ (C_{best} - 1)\\
&\qquad\quad else\\
&\qquad A_i = A_i + \emptyset_1\ x\ (C_{best})\\
&\quad end\ if\\
&\quad if\ rand\ () > 0.5\\
&\qquad C_i = C_i + \emptyset_2\ x\ (A_{best} - 1)\\
&\qquad\quad else\\
&\qquad C_i = C_i + \emptyset_2\ x\ (A_{best})\\
&\quad end\ if\\
&\quad if\ rand\ () < 0.5\\
&\qquad Re - initialized\ A_i\ and\ C_i\\
&\quad end\ if
\end{aligned} \quad (6)$$

This switching mechanism is what allows IMOA to steer past local optima and converge reliably on the global maximum power point in MPPT applications [16].

2.4. Particle swarm optimization (PSO)

PSO takes its cue from the foraging behavior of flocking birds or schooling fish: a population of particles, each a candidate solution, moves through the search space guided by both its own experience and that of the swarm as a whole [17], [18]. Applied to MPPT, each particle stands for a candidate duty cycle for the DC–DC converter, with the PV system's output power serving as the objective function to be maximized. Particle velocity is updated each iteration according to (7) [18], [19].

$$v_i^{k+1} = wv_i^k + c_1 r_1 \left(p_{best_i} - x_i^k\right) + c_2 r_2 \left(g_{best} - x_i^k\right) \quad (7)$$

Where v_i = velocity of particle iii, x_i = position of particle iii, w = inertia weight, $c_1 c_2$ = acceleration coefficients, $r_1 r_2$ = random numbers between 0 and 1, p_{best} = best position of particle iii, and g_{best} = global best position of the swarm. The particle position is then updated using:

$$x_i^{k+1} = x_i^k + v_i^{k+1} \quad (8)$$

Repeating this update step over successive iterations drives the swarm toward the optimum, which is how PSO tracks the PV system's maximum power point as irradiance changes [18], [19].

2.5. Optimization parameter settings and stopping criteria

To ensure the comparison between IMOA and PSO in section 3 is reproducible, both controllers were implemented as C-block routines in PSIM with the following settings. IMOA: a population of 5 candidate duty-cycle points, initialized at 16%, 32%, 48%, 64%, and 78%, was evolved over a maximum of 20 iterations. The first 50% of iterations formed the liquid (exploration) phase, in which each candidate duty cycle was pulled toward the best duty cycle found by that candidate so far (Abest) using an attraction coefficient af = 0.5; the remaining 50% formed the crystal (exploitation) phase, in which each candidate was pulled toward the global best duty cycle (Cbest) using a coefficient cf = 1.0, consistent with the two-stage search described in section 2.3. The duty cycle was bounded to 0-95% at every step to keep the SEPIC converter within continuous conduction mode. Once the maximum iteration count was reached, the controller held the duty cycle at Cbest and re-triggered the search from scratch whenever the measured output power deviated from the recorded best power by more than 1 W, indicating a change in irradiance.

The sampling interval was 30 ms. PSO: a population of 5 particles, initialized at duty cycles of 16%, 32%, 48%, 64%, and 80%, was evolved over a maximum of 10 iterations with a 20 ms sampling interval. The inertia weight w was re-randomized every iteration in the range [0, 0.5], and the cognitive and social acceleration coefficients were fixed at c1 = 0.8 and c2 = 0.8, each scaled by an independent random factor drawn from [0, 1] at every iteration, following the velocity update in (7). After the maximum iteration count was reached, the controller held the duty cycle at the global best and re-triggered the search, reinitializing the particles at 18%, 36%, 54%, and 72%, whenever the measured output power deviated from the recorded global best by more than 10 W.

2.6. Modeling SEPIC converter

A SEPIC was chosen as the power-conditioning stage because it can produce an output voltage above or below its input while keeping the output polarity unchanged, a feature well suited to photovoltaic applications where the panel's output voltage moves around with irradiance, temperature, and shading [19], [20], [21]. In this design, the SEPIC converter sits between the PV module and the load, with the MPPT controller setting its duty cycle to position the operating point. Adjusting that switching duty cycle is what lets the PV module track the MPP as environmental conditions change [19], [22], [23]. The ideal voltage conversion ratio of the SEPIC converter is expressed as (9).

$$\frac{V_o}{V_{in}} = \frac{D}{1-D} \quad (9)$$

Where V_o denotes the output voltage, V_{in} is its input voltage, and D is the switching duty cycle.

The (9) shows that the duty cycle directly sets the SEPIC converter's output voltage, which is exactly why this topology lends itself to MPPT control. Here, the duty cycle is continuously updated by the ion motion algorithm (IMOA) so that the system tracks the global maximum power point even when shading is uneven. To keep the SEPIC converter in continuous conduction mode (CCM), its inductor values are sized using (10).

$$L_1 = L_2 = \frac{V_{in} \cdot D}{\Delta I_L \cdot f_s} \quad (10)$$

Here, L_1 and L_2 denote the two inductances, ΔI_L is the inductor current ripple, and f_s denotes the switching frequency.

The coupling capacitor, which transfers energy between the input and output stages, can be sized approximately as (11).

$$C_1 = \frac{I_o \cdot D}{\Delta V_c \cdot f_s} \quad (11)$$

Where C_1 denotes the coupling capacitance, I_o is the output current, and ΔV_c is the allowed ripple in capacitor voltage. The output capacitor, used to limit voltage ripple at the output, can be estimated from (12).

$$C_o = \frac{I_o \cdot D}{\Delta V_o \cdot f_s} \quad (12)$$

Where C_o is the output capacitance and ΔV_o is the output voltage ripple.

In this design, the SEPIC converter forms the intermediate power-conversion link between the PV module and the load, with its switching signal generated by the IMOA-based MPPT controller, which keeps the PV module operating at the global maximum power point even when irradiance is non-uniform [20], [22]. Table 2 lists the component values of inductors, capacitors, the snubber network, and the switching frequency chosen for the SEPIC design to maintain stable CCM operation while minimizing voltage and current ripple during MPPT operation.

3. RESULTS AND DISCUSSION

Both IMOA and PSO were tested as MPPT controllers through closed-loop simulation in ALTAIR PSIM Professional 2022.1.0.8. The simulated system pairs a 100 Wp PV module with a SEPIC DC–DC converter, with the MPPT controller setting the converter's duty cycle to maximize harvested power as irradiance varies. This follows the same PV, SEPIC–MPPT arrangement described earlier, in which the optimization algorithm's duty-cycle output drives the converter. Figure 2 shows the closed-loop circuit built in ALTAIR PSIM, comprising two PV modules, a SEPIC converter, voltage and current sensors, a PWM driver, and the MPPT controller. The square C-block embeds the IMOA and PSO routines, which read the PV voltage and current, compute the instantaneous power, and output the duty-cycle reference that drives the SEPIC converter toward the maximum power point. Figure 4 compares the P–V curve under non-shading and partial-shading conditions. Without shading, the curve has one peak, a GMPP of 95.29 W, but under the three shading patterns, the GMPP falls to 37.32 W, 35.76 W, and 33.30 W, respectively, with local peaks clustering around 21 W. This illustrates how partial shading splits the curve into multiple peaks and makes locating the GMPP correspondingly harder.

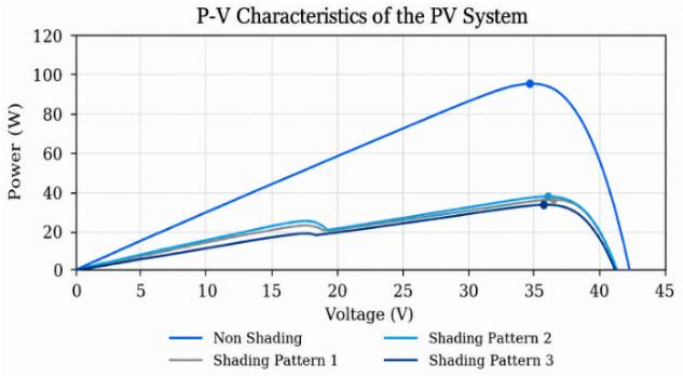

Figure 4. P-V characteristic of the PV system

Figure 5 plots the power-tracking response without shading. IMOA settles at 95.08 W, 99.77% accuracy, in 0.98 s, whereas PSO reaches only 93.83 W at 98.46% accuracy and takes a slower 1.99 s. IMOA

therefore converges faster and tracks more accurately than PSO when irradiance is uniform. Figure 6 covers shading pattern 1 (1000 and 750 W/m²). IMOA locates the GMPP at 37.27 W with 99.86% accuracy in 1.38 s, while PSO arrives at 37.13 W with 99.49% accuracy in 1.65 s; both reach the GMPP, but IMOA responds faster and tracks the reference power more tightly. Figure 7 presents the output power for shading pattern 2 (1000 and 500 W/m²). IMOA reaches 35.70 W at 99.83% accuracy in 1.32 s, compared with PSO's 35.65 W at 99.69% accuracy in 1.56 s, confirming that IMOA's tracking stays stable even as the shading deepens.

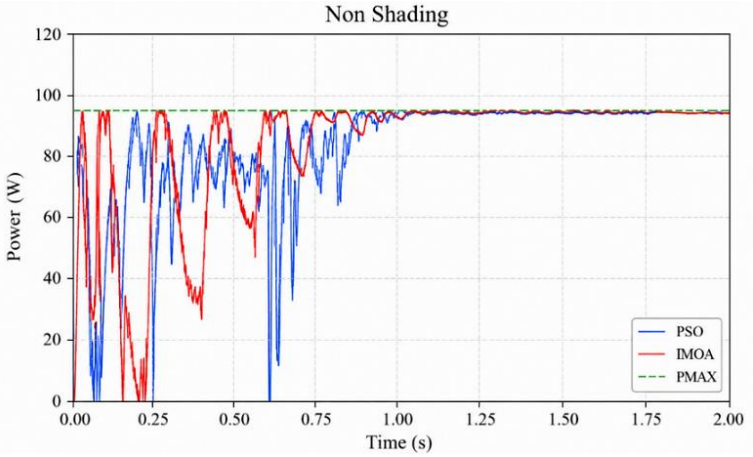

Figure 5. Comparison of IMOA and PSO in tracking under non-shading conditions

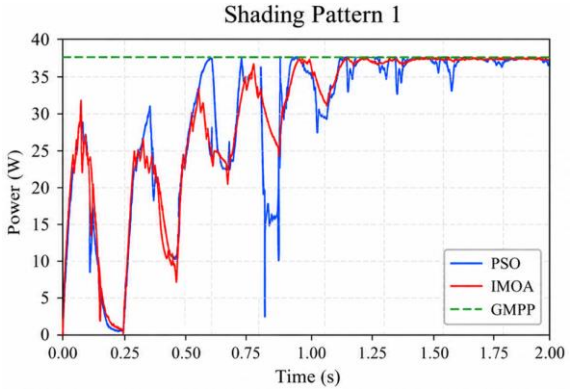

Figure 6. Comparison of IMOA and PSO in tracking under shading pattern 1

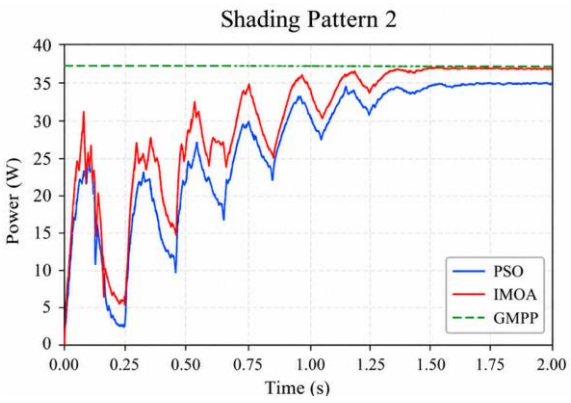

Figure 7. Comparison of IMOA and PSO in tracking under shading pattern 2

Figure 8 shows the response under the harshest shading tested (1000 and 250 W/m²). IMOA tracks the GMPP at 33.20 W with 99.69% accuracy in 1.50 s, while PSO reaches 33.11 W at 99.42% accuracy in 1.70 s - evidence that IMOA bypasses the nearby LMPP at roughly 21.44 W and still converges on the GMPP. Table 4 compares MPPT accuracy for IMOA and PSO across the test conditions. IMOA consistently comes out ahead, reaching as high as 99.77% under uniform irradiance, which speaks to its precision in stable conditions, and it keeps that accuracy above 99% even under partial shading, whereas PSO dips slightly, a sign of its greater susceptibility to local maxima. The gap suggests IMOA strikes a better exploration–exploitation balance and tracks the GMPP more reliably.

This advantage can be traced to the two-stage search mechanism described in section 2.3. During the liquid phase, IMOA's anions and cations are drawn toward the best-performing ion of the opposite charge across the whole search space (2)-(5), which lets the algorithm sample the region around each local peak in Table 3 broadly enough to avoid committing to a local maximum power point (LMPP) early in the search. Once the population stabilizes, the crystal phase in (6) narrows the search around the most promising ions, which is what shortens the tracking time relative to PSO in Table 4. PSO, by contrast, updates every particle's velocity each iteration using a single global-best term (7); when a local peak is discovered early, the swarm's global best can lock onto it, which is a widely reported cause of PSO's susceptibility to local maxima under partial

shading [16], [24]. This is consistent with the pattern in Table 4, where the accuracy gap between IMOA and PSO widens slightly as shading deepens from Partial Shading 1 to Partial Shading 3, since deeper shading produces LMPP that sit relatively closer in power to the GMPP and are therefore easier for a purely global-best-driven search to mistake for the true optimum. These results agree with the broader MPPT literature indicating that dual-mechanism or hybrid metaheuristics tend to outperform single-mechanism swarm methods precisely because they separate global exploration from local refinement [16], [25], and they extend that literature by showing the same pattern holds for IMOA specifically when paired with a SEPIC converter.

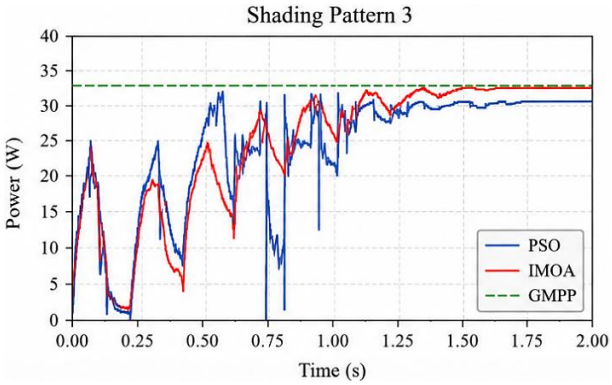

Figure 8. Comparison of IMOA and PSO in tracking under shading pattern 3

Table 4. Results of MPPT simulation accuracy comparison

Condition	Method	GMPP (W)	Pin (W)	Tracking time (s)	Accuracy (%)	Condition	Method	GMPP (W)	Pin (W)	Tracking time (s)	Accuracy (%)
Non-shading	IMOA	95.29	95.08	0.98	99.77	Partial shading 2	IMOA	35.76	35.70	1.32	99.83
	PSO	95.29	93.83	1.99	98.46		PSO	35.76	35.65	1.56	99.69
Partial shading1	IMOA	37.32	37.27	1.38	99.86	Partial shading 3	IMOA	33.30	33.20	1.50	99.69
	PSO	37.32	37.13	1.65	99.49		PSO	33.30	33.11	1.70	99.42

4. CONCLUSION

This work assessed an IMOA-based MPPT controller paired with a SEPIC converter for PV systems under both uniform and partially shaded irradiance. The simulations confirm that shading splits the P–V curve into multiple peaks, with the GMPP dropping from 95.29 W under uniform irradiance to 37.32 W, 35.76 W, and 33.30 W for shading patterns 1 through 3. Across every scenario tested, IMOA outperformed PSO in both tracking accuracy and convergence speed.

Under uniform irradiance, IMOA produced 95.08 W at 99.77% accuracy with a 0.98 s tracking time, and under shading, it kept accuracy at 99.86%, 99.83%, and 99.69% for Patterns 1 to 3 while converging faster than PSO throughout. Together, these results point to IMOA as an effective, dependable means of locating the GMPP and boosting power extraction as irradiance varies, and they suggest the approach has real promise for real-time PV applications and eventual hardware implementation with a SEPIC converter, pending the experimental validation outlined below.

This study has some limitations that should be acknowledged. First, the proposed controller was evaluated entirely through PSIM simulation; no hardware prototype or embedded-controller implementation was tested, so effects such as sensor noise, quantization, and computational delay on a real microcontroller remain unverified. Second, the partial-shading scenarios were limited to three static two-module irradiance patterns rather than dynamically changing or larger-array shading profiles, so the controller's behavior under rapidly fluctuating real-world conditions was not assessed. Third, IMOA's parameter settings (section 2.5) were fixed for this comparison and were not subjected to a sensitivity analysis, so their influence on the reported convergence time and accuracy is not yet fully characterized.

Future work will therefore focus on implementing the IMOA-based MPPT controller on an embedded microcontroller platform driving a physical SEPIC converter, validating its performance against the simulation results reported here under both static and dynamically changing partial-shading conditions, and examining its scalability to PV arrays with more than two modules. A sensitivity analysis of the IMOA population size and phase-transition threshold, together with a computational-cost comparison against PSO and other metaheuristic MPPT methods, would further clarify the practical trade-offs of adopting IMOA in real-time embedded applications.

ACKNOWLEDGMENTS

The authors thank Politeknik Elektronika Negeri Surabaya (PENS) for the facilities and support extended throughout this research and acknowledge the guidance and contributions of everyone involved in the study. It is hoped that these findings will help advance photovoltaic systems, MPPT technology, and renewable energy applications more broadly.

FUNDING INFORMATION

This work was self-funded by the authors as part of internal research activities, with technical and laboratory support provided by Politeknik Elektronika Negeri Surabaya (PENS).

AUTHOR CONTRIBUTIONS STATEMENT

This journal uses Contributor Roles Taxonomy (CRediT) to recognize individual author contributions, reduce authorship disputes, and facilitate collaboration.

Name of Author	C	M	So	Va	Fo	I	R	D	O	E	Vi	Su	P	Fu
Endro Wahjono	✓	✓	✓	✓		✓		✓	✓	✓	✓			✓
Indhana Sudiharto	✓	✓		✓	✓	✓	✓	✓	✓	✓		✓	✓	✓
Farah Izdihar Nakha Aqilah	✓	✓	✓		✓	✓		✓	✓	✓	✓		✓	

C : **C**onceptualization
M : **M**ethodology
So : **So**ftware
Va : **Va**lidation
Fo: **Fo**rmal analysis
I : **I**nvestigation
R : **R**esources
D : **D**ata Curation
O : Writing - **O**riginal Draft
E : Writing - Review & **E**diting
Vi : **Vi**sualization
Su : **Su**pervision
P : **P**roject administration
Fu : **Fu**nding acquisition

CONFLICT OF INTEREST STATEMENT

The authors declare no conflict of interest.

DATA AVAILABILITY

Data supporting these findings are contained within the article itself and its supplementary materials.

REFERENCES

[1] T. Esram and P. L. Chapman, "Comparison of photovoltaic array maximum power point tracking techniques," *IEEE Transactions on Energy Conversion*, vol. 22, no. 2, pp. 439–449, Jun. 2007, doi: 10.1109/TEC.2006.874230.
[2] N. Femia, G. Petrone, G. Spagnuolo, and M. Vitelli, "Optimization of perturb and observe maximum power point tracking method," *IEEE Transactions on Power Electronics*, vol. 20, no. 4, pp. 963–973, Jul. 2005, doi: 10.1109/TPEL.2005.850975.
[3] D. Sera, R. Teodorescu, and P. Rodriguez, "PV panel model based on datasheet values," in *2007 IEEE International Symposium on Industrial Electronics*, IEEE, Jun. 2007, pp. 2392–2396, doi: 10.1109/ISIE.2007.4374981.
[4] H. Patel and V. Agarwal, "Maximum power point tracking scheme for PV systems operating under partially shaded conditions," *IEEE Transactions on Industrial Electronics*, vol. 55, no. 4, pp. 1689–1698, Apr. 2008, doi: 10.1109/TIE.2008.917118.
[5] K. Ishaque and Z. Salam, "A review of maximum power point tracking techniques of PV system for uniform insolation and partial shading condition," *Renewable and Sustainable Energy Reviews*, vol. 19, pp. 475–488, Mar. 2013, doi: 10.1016/j.rser.2012.11.032.
[6] A. K. Abdelsalam, A. M. Massoud, S. Ahmed, and P. N. Enjeti, "High-performance adaptive perturb and observe MPPT technique for photovoltaic-based microgrids," *IEEE Transactions on Power Electronics*, vol. 26, no. 4, pp. 1010–1021, Apr. 2011, doi: 10.1109/TPEL.2011.2106221.
[7] T. Nagadurga, R. Devarapalli, and Ł. Knypiński, "Comparison of meta-heuristic optimization algorithms for global maximum power point tracking of partially shaded solar photovoltaic systems," *Algorithms*, vol. 16, no. 8, 2023, doi: 10.3390/a16080376.
[8] R. I. Jabbar, S. Mekhilef, M. Mubin, O. Alshammari, and A. Kazaili, "A fast MPPT method based on improved water cycle optimization algorithm for photovoltaic systems under partial shading conditions and load variations," *IEEE Open Journal of the Industrial Electronics Society*, vol. 5, pp. 1324–1338, 2024, doi: 10.1109/OJIES.2024.3510367.
[9] M. G. Villalva, J. R. Gazoli, and E. R. Filho, "Comprehensive approach to modeling and simulation of photovoltaic arrays," *IEEE Transactions on Power Electronics*, vol. 24, no. 5, pp. 1198–1208, May 2009, doi: 10.1109/TPEL.2009.2013862.
[10] R. W. Erickson and D. Maksimović, *Fundamentals of Power Electronics*. Springer Nature, 2020.
[11] H. Abu-Rub, M. Malinowski, and K. Al-Haddad, *Power Electronics for Renewable Energy Systems, Transportation and Industrial Applications*. John Wiley & Sons, 2014.
[12] O. Boubaker, "MPPT techniques for photovoltaic systems: a systematic review in current trends and recent advances in artificial intelligence," *Discover Energy*, vol. 3, no. 1, Dec. 2023, doi: 10.1007/s43937-023-00024-2.
[13] S. A. Sarang *et al.*, "Maximizing solar power generation through conventional and digital MPPT techniques: a comparative analysis," *Scientific Reports*, vol. 14, no. 1, Apr. 2024, doi: 10.1038/s41598-024-59776-z.
[14] W. A. Ahmed and M. A. Sharif, "Embedded MPPT for photovoltaic systems: low-cost microcontrollers, P&O and incremental conductance algorithms, and IoT-based monitoring — a systematic review," *NTU Journal of Renewable Energy*, vol. 10, no. 1, 2026.

[15] H. Abidi, L. Sidhom, and I. Chihi, "Systematic literature review and benchmarking for photovoltaic MPPT techniques," *Energies*, vol. 16, no. 8, Apr. 2023, doi: 10.3390/en16083509.
[16] M. L. Katche, A. B. Makokha, S. O. Zachary, and M. S. Adaramola, "A comprehensive review of maximum power point tracking (MPPT) techniques used in solar PV systems," *Energies*, vol. 16, no. 5, Feb. 2023, doi: 10.3390/en16052206.
[17] B. Javidy, A. Hatamlou, and S. Mirjalili, "Ions motion algorithm for solving optimization problems," *Applied Soft Computing*, vol. 32, pp. 72–79, Jul. 2015, doi: 10.1016/j.asoc.2015.03.035.
[18] T.-T. Nguyen, M.-J. Wang, J.-S. Pan, T. Dao, and T.-G. Ngo, "A load economic dispatch based on ion motion optimization algorithm," in *Advances in Intelligent Information Hiding and Multimedia Signal Processing*, 2020, pp. 115–125, doi: 10.1007/978-981-13-9710-3_12.
[19] J. Kennedy and R. Eberhart, "Particle swarm optimization," in *Proceedings of ICNN'95 - International Conference on Neural Networks*, IEEE, pp. 1942–1948, doi: 10.1109/ICNN.1995.488968.
[20] Y. Shi and R. Eberhart, "A modified particle swarm optimizer," in *1998 IEEE International Conference on Evolutionary Computation Proceedings. IEEE World Congress on Computational Intelligence (Cat. No.98TH8360)*, IEEE, 1998, pp. 69–73, doi: 10.1109/ICEC.1998.699146.
[21] M. Veerachary, "Power tracking for nonlinear PV sources with coupled inductor SEPTIC converter," *IEEE Transactions on Aerospace and Electronic Systems*, vol. 41, no. 3, pp. 1019–1029, Jul. 2005, doi: 10.1109/TAES.2005.1541446.
[22] H. Rezk, A. Fathy, and A. Y. Abdelaziz, "A comparison of different global MPPT techniques based on meta-heuristic algorithms for photovoltaic system subjected to partial shading conditions," *Renewable and Sustainable Energy Reviews*, vol. 74, pp. 377–386, Jul. 2017, doi: 10.1016/j.rser.2017.02.051.
[23] S. Buso and P. Mattavelli, "Digital control in power electronics," *Synthesis Lectures on Power Electronics*, vol. 1, no. 1, pp. 1–158, Jan. 2006, doi: 10.2200/S00047ED1V01Y200609PEL002.
[24] K. Ishaque, Z. Salam, M. Amjad, and S. Mekhilef, "An improved particle swarm optimization (PSO)–based MPPT for PV with reduced steady-state oscillation," *IEEE Transactions on Power Electronics*, vol. 27, no. 8, pp. 3627–38, 2012, doi: 10.1109/TPEL.2012.2185713.
[25] A. Safari and S. Mekhilef, "Simulation and hardware implementation of incremental conductance MPPT with direct control method using cuk converter," *IEEE Transactions on Industrial Electronics*, vol. 58, no. 4, pp. 1154–1161, 2011, doi: 10.1109/TIE.2010.2048834.

BIOGRAPHIES OF AUTHORS



Endro Wahjono is a lecturer in the Department of Industrial Electrical Engineering at Politeknik Elektronika Negeri Surabaya (PENS), Surabaya, Indonesia. His teaching and research activities focus on electrical engineering, particularly renewable energy systems and industrial electrical applications. His research interests include power electronics, electric drives, photovoltaic systems, renewable energy systems, and industrial control systems. He has contributed to scientific publications on photovoltaic power generation, maximum power point tracking (MPPT) techniques, and renewable energy applications. He is also involved in applied research and engineering projects related to electrical energy conversion systems. He can be contacted at email: endro@pens.ac.id.



Indhana Sudiharto was born in Madiun, Indonesia, in 1966. He received his Bachelor of Engineering degree in power systems from Institut Teknologi Sepuluh Nopember, Surabaya, Indonesia, in 1996, and his Master of Engineering degree in power systems from the same institution in 2006. He is currently an associate professor in the Department of Electrical Engineering at Politeknik Elektronika Negeri Surabaya (PENS), Indonesia. He joined the Division of Industrial Electrical Engineering, Department of Electrical Engineering, PENS, as a lecturer in 1996. He leads the Power Quality research group at PENS. His research interests include power systems, renewable energy, and power electronics. His teaching areas include electrical measurement and instrumentation, electrical power system protection, and power quality. He can be connected at email: indhana@pens.ac.id or indhanasudiharto@gmail.com.



Farah Izdihar Nakha Aqilah is a final-year student in the Department of Industrial Electrical Engineering at Politeknik Elektronika Negeri Surabaya (PENS), Indonesia. Her research interests include renewable energy systems, photovoltaic systems, power electronics, maximum power point tracking (MPPT) techniques, and embedded control systems. She has been involved in several projects related to SEPIC converters and photovoltaic energy conversion systems. She is proficient in engineering software, including MATLAB, ETAP, STM32CubeIDE, Proteus, and AutoCAD. She can be contacted at email: nakhafarah@gmail.com.